Chapter 4:
Reduction of Hardened pellets by solid reductants

4.1. Introduction

When a metal oxide (MO) reacts with a suitable reducing agent (a chemical species either in gas or solid form) under appropriate conditions, it yields metal (M) and the oxide of the reducing agent (RO), as represented by the equation: $MO + R \rightarrow M + RO$. The selection of the reducing agent, R, is crucial, with a key criterion being that the standard free energy of formation (ΔG°) of the resulting compound RO should be more negative than that of the metal oxide MO, ensuring thermodynamic feasibility [89]. In the reduction of iron oxides, common reagents such as carbon, hydrogen, and carbon monoxide are employed because their resulting oxides exhibit greater thermodynamic stability compared to iron oxides, as evidenced by their more negative ΔG° values.

This chapter provides a detailed examination of reduction studies conducted on hardened MMO pellets using solid reductants like non coking coal and coke. The objective was to optimize the time and temperature conditions for the carbothermic reduction process. The pellets, comprising 1.5 wt.% colemanite, were subjected to reduction in the temperature range of 950–1150°C for durations spanning from 30 to 120 mins. XRD and SEM analysis of reduced pellets were conducted to determine the phase and morphological changes occurred during reduction. A significant observation was the absence of the chromite phase in reduced MMO pellets after 1100°C, indicating complete separation of chromium oxide and iron oxide. In section 3.5 of the preceding chapter, it was noted that the induration process of the pellets led to the conversion of chromite into a complex sesquioxide. This transformation notably improved the reducibility of the chromite phase within the pellets [19]. Additionally, the chapter explores studies focused on understanding the reduction kinetics of the hardened MMO pellets. Efforts were also made to determine the activation energy for the carbothermic reduction of MMO pellets.

4.2. Results and Discussion

4.2.1. Visual Observation

Figures 4.1 and **4.2** show the variation in size and colour of pellets reduced with non coking coal and coke respectively, with respect to change in reduction time and temperature.

The colour of the pellets changed from black to a blackish brown with the rise in

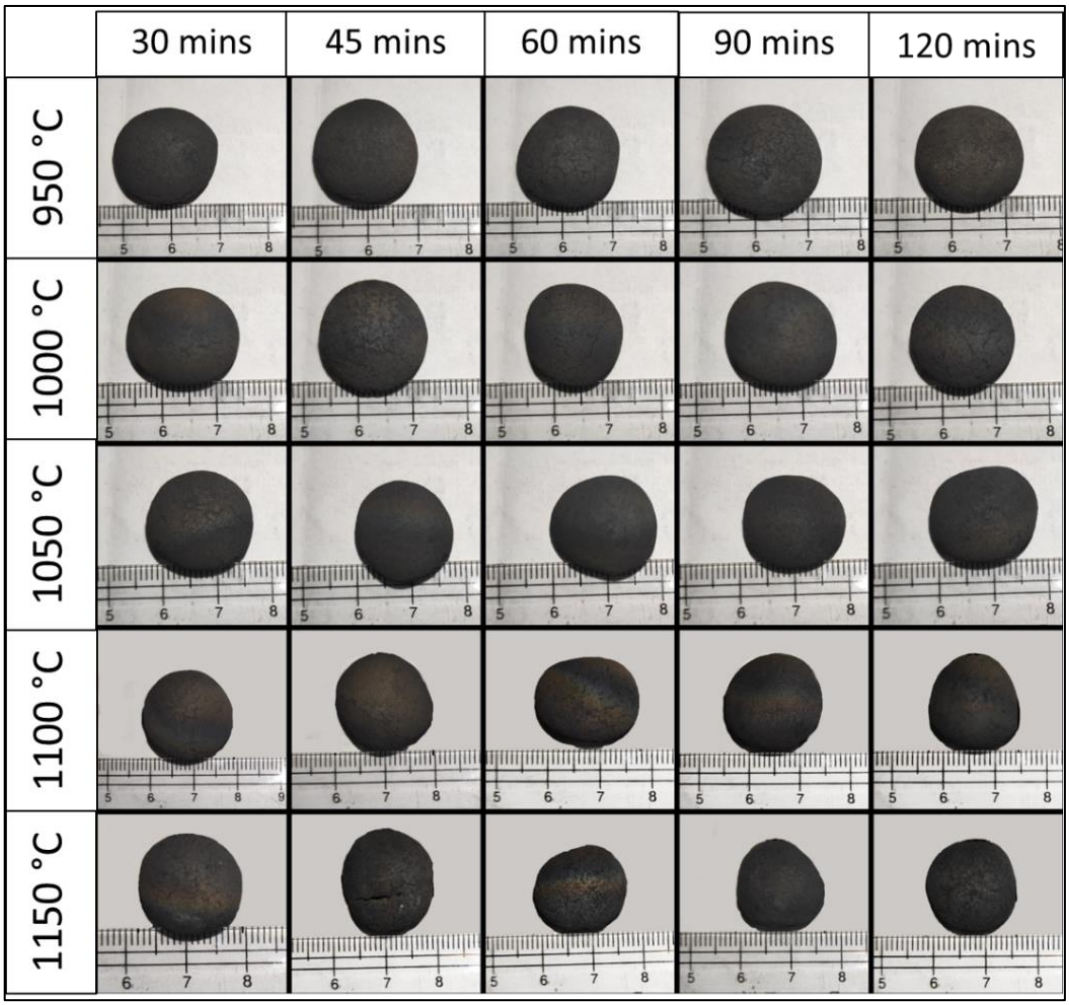

Figure 4.1: Variation in appearance of non-coking coal reduced pellets with change in reduction temperature and time

reduction temperature. This brownish colour resulted from the formation of magnetite at temperatures above 1050°C. At higher temperatures, a bluish tinge was also observed. Reduced iron ore pellets may display a bluish tinge due to the formation of a thin layer of magnetite on their surface. This color variation, ranging from deep blue to

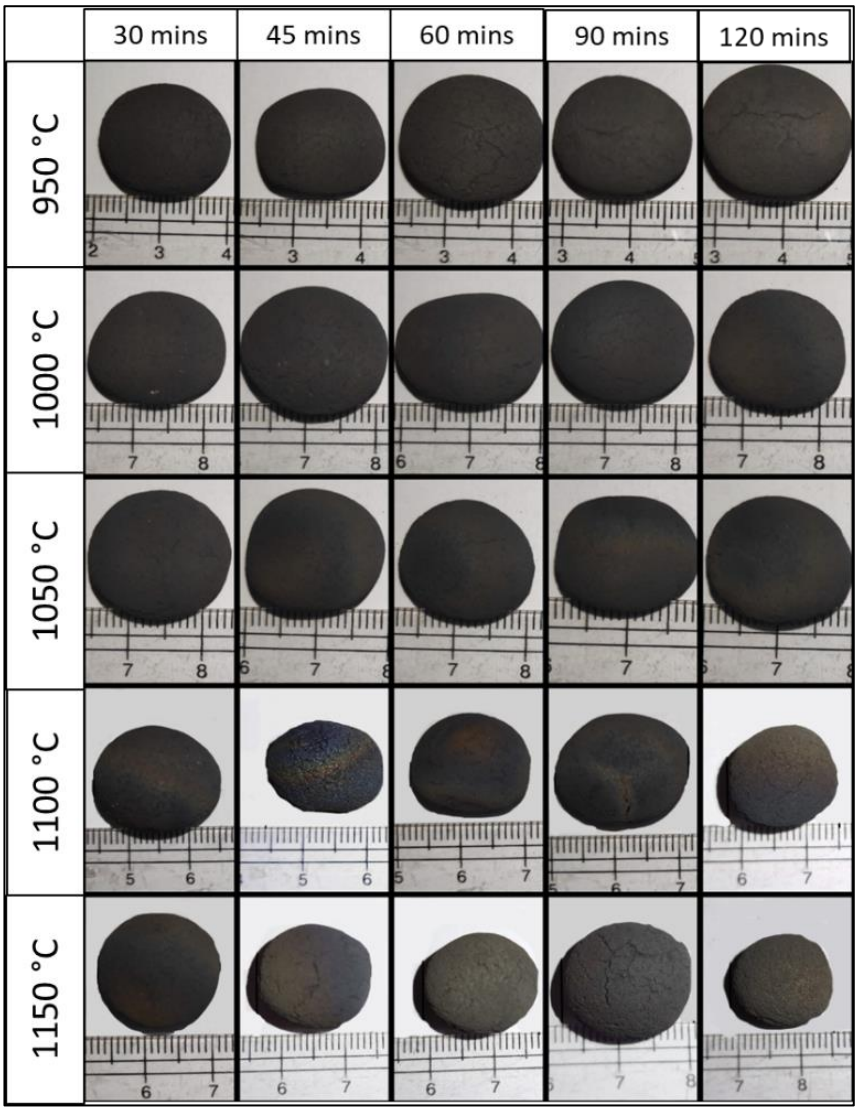

Figure 4.2:Variation in appearance of coke reduced pellets with change in reduction temperature and time

brownish black, is typically observed in magnetite due to the presence of both Fe^{2+} and Fe^{3+} ions. The movement of electrons between the anions usually leads to selective absorption of light in oxides containing metals in different valence states [90]. This colour variation depends on the thickness of the magnetite layer and the angle of incident light. Therefore, the bluish tinge is not visible on every pellet reduced at temperatures of 1100 °C and 1150 °C; instead, mostly a blackish-brown color was observed (**Figure 4.1 and 4.2**).

Minor shrinkage of pellets was also observed at temperatures above 1100 °C. This shrinkage was due to the sintering of the metallic phase and consolidation of pellets that usually occur at such temperatures [91, 92].

4.2.2. Reduction Studies

Carbothermic reduction of the hardened MMO pellets was carried out according to the methods mentioned in Section 2.6.1. The MMO pellet's weight before and after reduction were recorded to calculate the weight change. The weight change of the pellets was used to calculate the Degree of Reduction (% R) as

%R = (Change in wt. of pellet/ Wt. of removable oxygen present in Initial pellet) × 100…….(4.1)

The weight of removable oxygen was determined by considering the oxygen associated with the oxides in the MMO pellets, which can be readily reduced by carbon (C) or carbon monoxide (CO) within the temperature range of 950-1150°C. A negative ΔG_r of the reduction reaction within the specified temperature range indicates spontaneous reduction of the oxide. The ΔG_r for NiO, Fe_2O_3, Fe_3O_4, and FeO reduction by carbon at 950 °C is -134 KJ, -243.14 KJ, -30.79 KJ, and -25 KJ, respectively, and ΔG_r for Fe_2O_3, Fe_3O_4 and FeO reduction by CO at 950 °C is -99.76, -8.892 and 8.97 KJ respectively, calculated using FactSage software [93]. Cr is present in the form of a sesquioxide in the hardened MMO pellets (**Figure 3.7**). This sesquioxide exhibits better reducibility compared to chromite. Chromite is reducible by CO from 1028°C onwards, when the $CO/(CO+CO_2)$ % in the reducing gas exceeds 93% [20]. It was very probable that this specified condition was met during the experimentation as the ΔGr for the reaction "CO_2+ C ←→ 2 CO" is -56.55 KJ at 1028°C [93]. Consequently, the pellets contain approximately 19.6 wt.% of removable oxygen (associated with Fe, Cr and Ni). Therefore, equation 4.1 can be rewritten as follows

%R= (Change in wt. of pellet/ 0.196 × initial wt. of pellet) × 100…….(4.2)

The results of the reduction studies with non coking coal and coke are shown below in **Tables 4.1 and 4.2** respectively.

Table 4.1: Percentage Reduction (%R) of pellets reduced with non coking coal

Temp (°C)	Time (mins)	Initial wt. of pellet (gm)	Final Wt. of pellets (gm)	Wt. loss (gm)	Initial wt. of removable oxygen in pellet (gm)	% R
950	30	7.734	7.326	0.408	1.516	26.94
	45	8.298	7.711	0.587	1.626	36.12
	60	8.152	7.420	0.732	1.598	45.81
	90	8.269	7.430	0.839	1.621	51.76
	120	6.831	6.122	0.709	1.339	52.95
1000	30	6.943	6.291	0.652	1.361	47.92
	45	7.899	7.060	0.839	1.548	54.19
	60	6.98	6.185	0.795	1.368	58.08
	90	8.341	7.305	1.036	1.635	63.39
	120	7.5	6.467	1.033	1.470	70.3
1050	30	6.968	6.205	0.763	1.366	55.85
	45	6.619	5.751	0.868	1.297	66.89
	60	7.822	6.783	1.039	1.533	67.79
	90	6.569	5.589	0.980	1.288	76.08
	120	7.683	6.493	1.190	1.506	79.05
1100	30	8.347	7.437	0.910	1.636	55.63
	45	7.366	6.399	0.967	1.444	66.98
	60	6.737	5.776	0.961	1.320	72.79
	90	7.837	6.652	1.185	1.536	77.12
	120	6.506	5.480	1.026	1.275	80.44
1150	30	6.267	5.459	0.808	1.228	65.79
	45	7.975	6.887	1.088	1.563	69.63
	60	6.349	5.429	0.920	1.244	73.92
	90	6.862	5.860	1.002	1.345	74.48
	120	6.727	5.719	1.008	1.318	76.48

Table 4.2: Percentage Reduction (%R) of pellets reduced with coke

Temp (°C)	Time (mins)	Initial wt. of pellet (gm)	Final Wt. of pellets (gm)	Wt. loss (gm)	Initial wt. of removable oxygen in pellet (gm)	% R
950	30	5.848	5.495	0.353	1.146	30.75
	45	6.034	5.610	0.424	1.183	35.83
	60	8.361	7.690	0.671	1.639	40.97
	90	7.04	6.382	0.658	1.380	47.67
	120	9.306	8.427	0.879	1.824	48.21
1000	30	5.62	5.174	0.446	1.102	40.48
	45	7.533	6.842	0.691	1.476	46.77
	60	7.047	6.339	0.708	1.381	51.25
	90	7.222	6.384	0.838	1.416	59.2
	120	5.011	4.375	0.636	0.982	64.73
1050	30	6.352	5.701	0.651	1.245	52.34
	45	7.097	6.197	0.900	1.391	64.67
	60	6.145	5.336	0.809	1.204	67.17
	90	5.484	4.741	0.743	1.075	69.09
	120	6.738	5.800	0.938	1.321	70.99
1100	30	7.677	6.725	0.952	1.505	53.24
	45	6.206	5.396	0.810	1.216	66.61
	60	6.703	5.792	0.911	1.314	69.34
	90	7.625	6.493	1.132	1.495	75.76
	120	7.676	6.530	1.146	1.504	76.18
1150	30	6.628	5.751	0.877	1.299	67.54
	45	8.085	6.979	1.106	1.585	69.77
	60	7.385	6.356	1.029	1.447	71.07
	90	6.802	5.844	0.958	1.333	71.88
	120	6.93	5.943	0.987	1.358	72.65

The metallization in pellets (%Fe_M) was calculated according to the methods mentioned in Section 2.6.3 of Chapter 2 and is shown in **Tables 4.3** and **4.4** for non coking coal and coke.

Table 4.3 :Percentage metallization (% Fe_M) of pellets reduced with non coking coal

Temp (°C)	Time (mins)	Initial wt. of pellet (gm)	Wt. of DRI (gm)	Initial wt. of Iron in pellet (gm)	Fe per gm DRI, Fe(T) (gm)	$K_2Cr_2O_7$ Solution consumed (ml)	Fe(M) (gm)	Fe_M (%)
950	30	7.734	7.326	3.488	0.476	17.5	0.033	6.842
	45	8.298	7.711	3.742	0.485	33.4	0.062	12.830
	60	8.152	7.42	3.677	0.495	63.7	0.119	23.949
	90	8.269	7.43	3.729	0.502	92.2	0.172	34.212
	120	6.831	6.122	3.081	0.503	114.2	0.213	42.252
1000	30	6.943	6.291	3.131	0.498	107.5	0.200	40.199
	45	7.899	7.06	3.562	0.505	133.0	0.248	49.095
	60	6.98	6.185	3.148	0.509	161.3	0.300	59.016
	90	8.341	7.305	3.762	0.515	175.0	0.326	63.293
	120	7.5	6.467	3.383	0.523	209.5	0.390	74.583
1050	30	6.968	6.205	3.143	0.506	111.7	0.208	41.055
	45	6.619	5.751	2.985	0.519	133.5	0.249	47.897
	60	7.822	6.783	3.528	0.520	177.3	0.330	63.464
	90	6.569	5.589	2.963	0.530	225.0	0.419	79.030
	120	7.683	6.493	3.465	0.534	242.7	0.452	84.675
1100	30	8.347	7.437	3.764	0.506	140.9	0.262	51.832
	45	7.366	6.399	3.322	0.519	173.6	0.323	62.266
	60	6.737	5.776	3.038	0.526	227.1	0.423	80.399
	90	7.837	6.652	3.534	0.531	242.8	0.452	85.097
	120	6.506	5.48	2.934	0.535	260.6	0.485	90.373
1150	30	6.267	5.459	2.826	0.518	154.6	0.288	55.595
	45	7.975	6.887	3.597	0.522	182.3	0.339	65.003
	60	6.349	5.429	2.863	0.527	230.2	0.429	81.254
	90	6.862	5.86	3.095	0.528	235.8	0.439	83.136
	120	6.727	5.719	3.034	0.530	243.7	0.454	85.531

Table 4.4: Percentage metallization (% Fe_M) of pellets reduced with coke

Temp (°C)	Time (mins)	Initial wt. of pellet (gm)	Wt. of DRI (gm)	Initial wt. of Iron in pellet (gm)	Fe per gm DRI, Fe(T) (gm)	$K_2Cr_2O_7$ Solution consumed (ml)	Fe(M) (gm)	Fe_M (%)
950	30	5.848	5.495	2.637	0.480	15.3	0.028	5.925
	45	6.034	5.61	2.721	0.485	27.2	0.051	10.458
	60	8.361	7.69	3.771	0.490	47.6	0.089	18.081
	90	7.04	6.382	3.175	0.497	71.1	0.132	26.620
	120	9.306	8.427	4.197	0.498	89.2	0.166	33.344
1000	30	5.62	5.174	2.535	0.490	81.4	0.151	30.923
	45	7.533	6.842	3.397	0.497	91.1	0.170	34.147
	60	7.047	6.339	3.178	0.501	105.9	0.197	39.344
	90	7.222	6.384	3.257	0.510	148.1	0.276	54.042
	120	5.011	4.375	2.260	0.517	182.3	0.339	65.714
1050	30	6.352	5.701	2.865	0.502	119.6	0.223	44.305
	45	7.097	6.197	3.201	0.516	145.6	0.271	52.502
	60	6.145	5.336	2.771	0.519	168.2	0.313	60.293
	90	5.484	4.741	2.473	0.522	202.7	0.377	72.346
	120	6.738	5.8	3.039	0.524	214.6	0.400	76.254
1100	30	7.677	6.725	3.462	0.515	141.2	0.263	51.082
	45	6.206	5.396	2.799	0.519	179.0	0.333	64.241
	60	6.703	5.792	3.023	0.522	192.9	0.359	68.807
	90	7.625	6.493	3.439	0.530	222.0	0.413	78.031
	120	7.676	6.53	3.462	0.530	238.1	0.443	83.61
1150	30	6.628	5.751	2.989	0.520	167.9	0.313	60.135
	45	8.085	6.979	3.646	0.522	186.7	0.348	66.543
	60	7.385	6.356	3.331	0.524	208.8	0.389	74.188
	90	6.802	5.844	3.068	0.525	214.9	0.400	76.215
	120	6.93	5.943	3.125	0.526	217.3	0.405	76.952

4.2.3. Effect of reductant on % R and % Fe_M

The effect of reductant on % R and % Fe_M can be understood by plotting the values of % R and % Fe_m obtained in **Tables 4.1, 4.2, 4.3,** and **4.4** against reduction time The plots are shown in **Figure 4.3.**

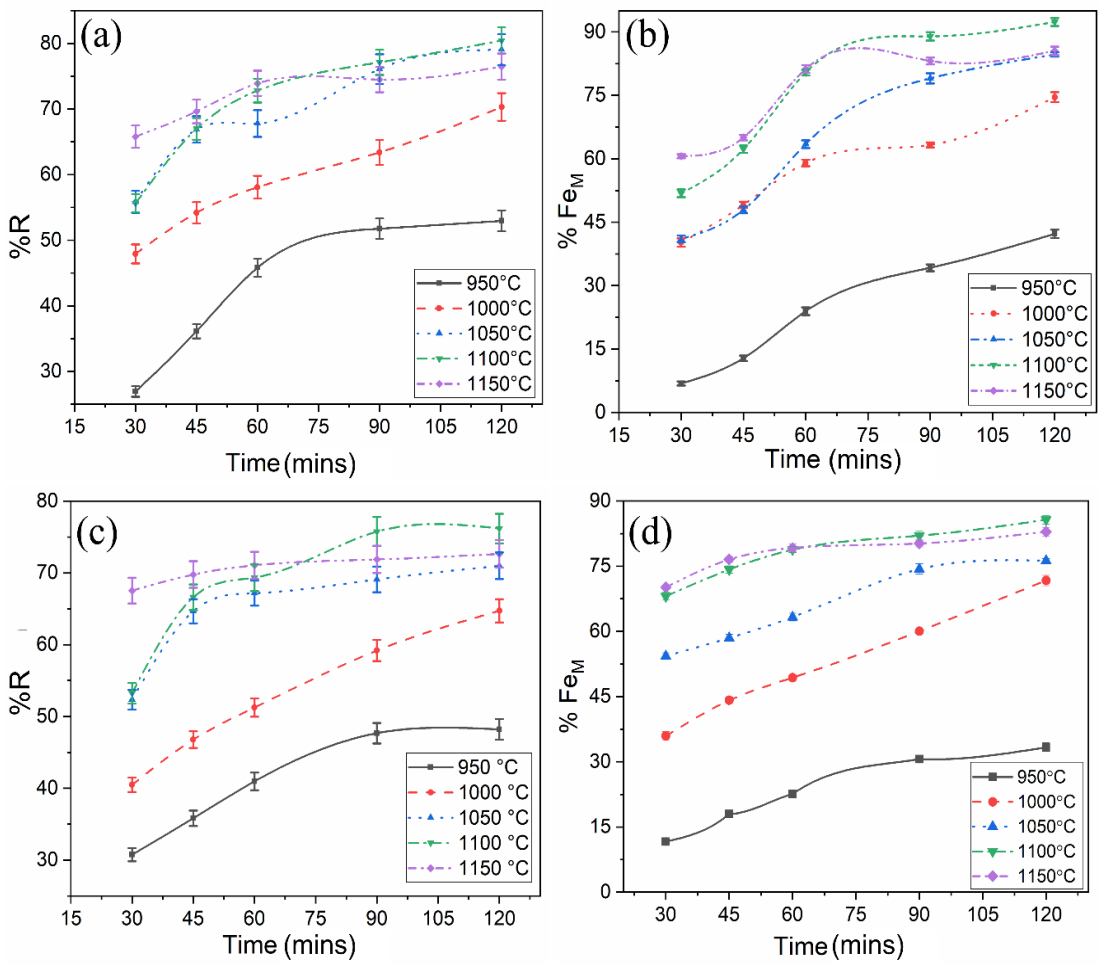

Figure 4.3:(a) %R and (b) %Fe_M of pellets reduced with non-coking coal; (c) %R and (d) %Fe_M of pellets with reduced with coke at different time-temperature combinations

In general, % R and % Fe_M were found to increase with an increase in temperature and reduction time. Maximum % R of 80% and % Fe_M of 90% were obtained at 1100 °C and a reduction time of 120 mins when noncoking coal was used as a reductant. Similarly, a maximum % R of 76% and a % Fe_M of 83% was obtained at 1100 °C and a reduction time of 120 mins when coke was used as a reductant. In contrast a maximum % R of about 55% was obtained by reducing 8mm MMO lumps at 1100 °C for 120 mins [10]. Thus, pelletization improved the solid based reduction of MMO.

Non-coking coal was a better reductant owing to the higher % R and % Fe_M obtained at almost all time-temperature combinations. The slight decrease in % R values could be due to the lower total carbon in coke (57%) as compared to noncoking coal (69%). The lower carbon and volatile matter content was the reason for the lower reducibility obtained with coke. The volatile matter contains hydrocarbons, which, on decomposition, give rise to hydrogen and carbon monoxide, contributing in the reduction process [94].

4.2.4. Effect of time and temperature on % R and % Fe_M

An interesting phenomenon was observed when the reduction time was increased for pellets reduced at both 1100 °C and 1150 °C with non-coking coal. Until 60 mins of reduction time, the % R and % Fe_M was more for pellets reduced at 1150 °C than for pellets reduced at 1100 °C beyond which, the % R and % Fe_M became constant for pellets reduced at 1150 °C while it continuously increased for pellets reduced at 1100 °C (**Figure 4.3a and 4.3b**). Similar behaviour was also observed when coke was used as a reductant. The % R and % Fe_M at 1100 °C were more than the reduction at 1150 °C after about 90 mins (**Figure 4.3c and 4.3d**). The % Fe_M for pellets reduced at 1150 °C increased initially from 30 min to 45 mins, after which it became almost constant. Therefore, there seems to be some hindrance to reduction at higher temperatures, irrespective of the reductant used. The abnormal behaviour was due to the shrinkage of pellets. Sintering of grains at higher temperatures often leads to shrinkage which might have reduced the diffusion of reducing gases into the pellet and hindered the reduction reaction[18, 91]. The shrinkage of pellets can be observed in **Figure 4.4** for non coking coal reduced pellets and **Figure 4.5** for coke reduced pellets. The diameter shown in **Figure 4.4** is only indicative. The actual % apparent volume change was calculated by taking the average pellet diameter measured from eight orientations. When non coking

coal was used, the shrinkage was more drastic in the case of pellets reduced at 1150 °C than in pellets reduced at 1100 °C. This shrinkage was found to increase with increasing reduction time. This can be correlated with **Figure 4.3a**, where the % R became constant from 60 mins onwards for pellets reduced at 1150 °C. In the case of pellets reduced at 1100 °C, the shrinkage is almost similar on increasing reduction time from 60 mins to 90 mins (**Figure 4.3**). Thus % R continued to increase even beyond 60 mins. This shrinkage decreased porosity, thereby restricting the inward flow of reducing gas for further reduction reaction inside the pellet.

Temp	Time	30 mins	45 mins	60 mins	90 mins	120 mins
1100 °C	Before reduction	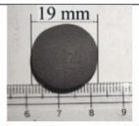	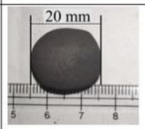	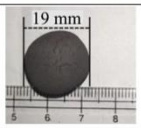	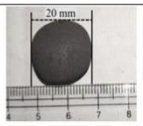	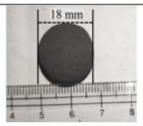
	After reduction	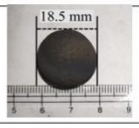	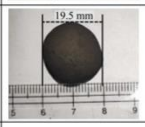	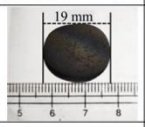	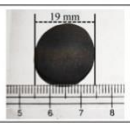	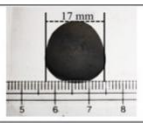
	% apparent volume change	-3.11	-5.27	-5.71	-7.85	-8.06
1150 °C	Before reduction	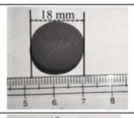	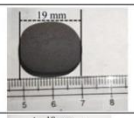	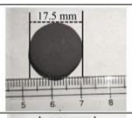	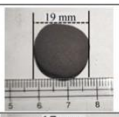	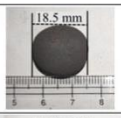
	After reduction	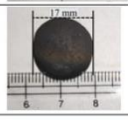			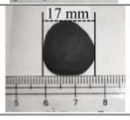	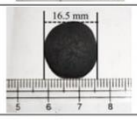
	% apparent volume change	-11.49	-10.83	-11.09	-16.65	-19.24

Figure 4.4: Photographs of non-coking coal reduced pellets depicting shrinkage at 1100°C and 1150 °C for different reduction time.

A similar behaviour was observed when coke was used as a reductant. The observed shrinkage was more severe at 1150 °C than at 1100 °C. Again, the diameter shown in **Figure 4.5** is only indicative. The actual % apparent volume change was calculated by taking the average pellet diameter measured from eight orientations. This can be correlated with **Figure 4.3c** wherein the % R at 1150 °C does not increase much with increase in time, while the % R at 1100 °C keeps continuously increasing till 90 mins. In this case too, the increased shrinkage with rise in temperature and reduction time led

to reduced porosity which in turn reduced the penetration of reducing gases into the pellet. Generation of new slag phases and sintering could be the reason for the observed shrinkage of pellets. Both the above mentioned factors have been investigated in the following subsections.

Temp	Time	30 mins	45 mins	60 mins	90 mins	120 mins
1100 °C	Before reduction	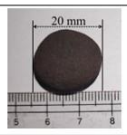			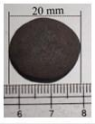	
	After reduction					
	% apparent volume change	0.36	-3.25	-5.66	-7.44	-8.03
1150 °C	Before reduction					
	After reduction					
	% apparent volume change	-10.54	-11.7	-14.24	-15.3	-20.61

Figure 4.5: Photographs of coke reduced pellets depicting shrinkage at 1100°C and 1150°C for different reduction time

4.2.4.1. XRD studies

XRD analysis of the pellets reduced at 1100 °C and 1150 °C for 60 mins and 90 mins with non-coking coal (**Figure 4.6**) and coke (**Figure 4.7**) were done to get insights into any phases that may have hindered the reduction at 1150 °C

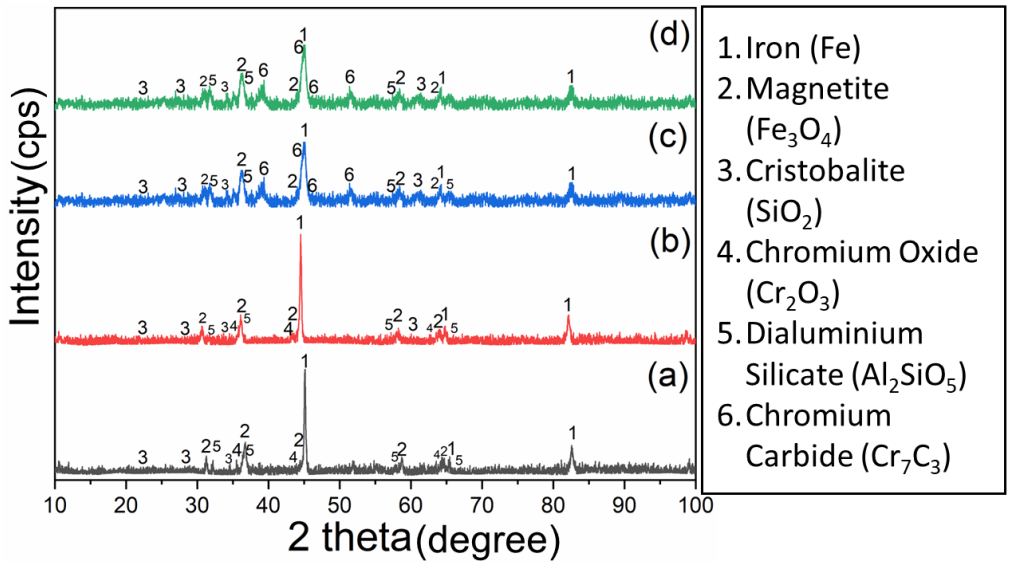

Figure 4.6: XRD analysis of pellet reduced with non-coking coal at (a) 1100 °C for 60 mins; (b) 1100 °C for 90 mins; (c) 1150 °C for 60 mins; and (d) 1150 °C for 90 mins.

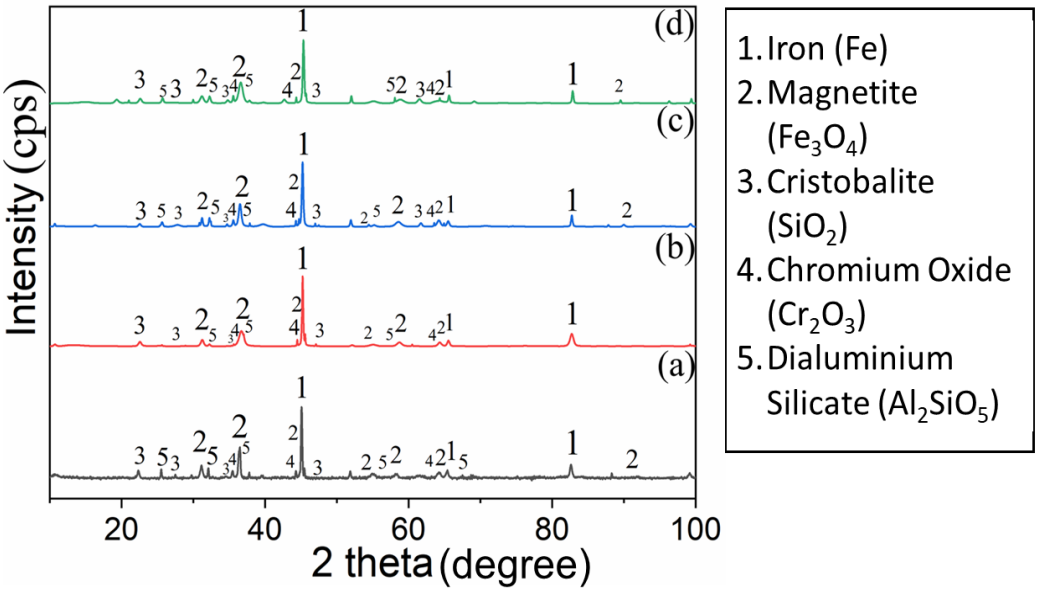

Figure 4.7: XRD analysis of pellet reduced with coke at (a) 1100 °C for 60 mins; (b) 1100 °C for 90 mins; (c) 1150 °C for 60 mins; and (d) 1150 °C for 90 mins.

Iron (Fe) was the major phase present at both 1100 °C and 1150 °C (**Figure 4.6 and 4.7**). At tempertaures above 950 °C, iron oxides are indirectly reduced by CO. The CO

is produced when C reacts with CO_2 (boudouard reaction) The transformation of hematite to iron (Fe) in the temperature range of 950-1150°C according to the following reactions [17]

$C + O_2(g) \Leftrightarrow CO_2(g)$ ΔG_r= -396.09 KJ to -396.18 KJ……(4.3)

$CO_2(g) + C \Leftrightarrow 2\,CO(g)$ ΔG_r= -43.05 KJ to -77.98 KJ……(4.4)

$Fe_2O_3 + 3CO\,(g) \Leftrightarrow Fe + 3CO_2(g)$ ΔG_r= -23.06 KJ to -20.91 KJ……(4.5)

The other significant phases present at both 1100 °C and 1150 °C are magnetite (Fe_3O_4), cristobalite (SiO_2) and dialuminium silicate (Al_2SiO_5) (**Figure 4.6 and 4.7**). Magnetite is also a product of the indirect reduction of hematite by CO in the temperature range of 950-1150°C which happens acccording to the following reaction:

$3\,Fe_2O_3 + CO\,(g) \Leftrightarrow 2\,Fe_3O_4 + CO_2(g)$ ΔG_r= -110.40 KJ to -121.66 KJ…(4.6)

The sole phase change observed when increasing the temperature from 1100 °C to 1150 °C is the transformation of chromium oxide (Cr_2O_3) to chromium carbide (Cr_7C_3) in pellets reduced with non-coking coal (**Figure 4.6**). However, this particular phase change is usually seen at 1150°C which happens according to the following reaction [14, 95].

$7\,Cr_2O_3 + 27\,C\,(g) \Leftrightarrow 2\,Cr_7C_3 + 21\,CO(g)$ ΔG_r=-45.72 KJ……(4.7)

This phase change was not observed when coke was used as reductant. Chromium oxide (Cr_2O_3) was visible at both 1100 °C and 1150 °C (**Figure 4.7**). This was due to the lower carbon content of coke when compared to non-coking coal. Since the reductant (non-coking coal or coke) was the only source of carbon in the system, the amount of carbon in coke was not sufficient enough for both reduction of chromite and carburization of Cr_2O_3. Non coking coal also contained higher amount of VM than coke, which decompose to form hydrogen and carbon monoxide thereby enhancing the reducing power of non-coking coal.

It was very interesting to note that magnetite was still present even at 1150 °C along with chromium carbide (**Figure 4.6**) which indicated that the reduction of chromium oxides and iron oxides had happened simultaneously. It was in contrast to a summary of previous studies [21] which had described iron oxides to be reducing much earlier than chromium oxides. Oxidation of chromite to sesquioxide during hardening may have contributed to the enhanced reducibility of the chromium oxides. This conversion occurs by oxidation of Fe^{2+} to Fe^{3+} in the chromite spinel resulting in the formation of a complex sesquioxide solid solution ($(FeCr)_2O_3$) [96, 97]. The Fe^{2+} ions on the surface of the chromite grain get oxidized to Fe^{3+} first and then the high oxygen potential present during hardening of pellets, leads to outward diffusion of Fe^{2+} ions from the tetrahedral sites in the core of the chromite grains to the solid-gas interface at the surface of the grain for further oxidation. This results in creation of a large amount of vacancies at the tetrahedral sites in the chromite spinel, thereby increasing the reactivity of the chromite spinel. All the Fe ions become concentrated near the surface of the chromite grain, which leads to enhanced reducibility of chromite during reduction [19]. Thus the sesquioxide ($(Fe,Cr)_2O_3$) may get reduced at temperature lower than or at 1027 °C, which is the temperature at which chromite ($FeCr_2O_4$) starts getting reduced by CO to Fe and Cr_2O_3 [20] according to the reaction:

$$FeCr_2O_4 + CO\ (g) \Leftrightarrow Fe + Cr_2O_3 + CO_2(g) \quad \text{.....(4.8)}$$

Therefore, the Cr_2O_3 phase was visible in pellets reduced with non coking coal at 1100 °C (**Figure 4.6 and 4.7**). The binder used, i.e., colemanite contains borate and lime as the major constituents and its presence might have contributed towards higher reactivity of chromite as also noted before by other researchers [23-26].

Neither there was a significant phase change, nor formation of new slag phases when the reduction temperature was increased. The presence of slag phases could have

indicated a possible reduction in the pellets' porosity, which would have lowered the penetration of reducing gases into the pellet core and decreased reducibility.

4.2.4.2. SEM study of pellets

Pellets reduced with both non coking coal and coke for 60 mins and 90 mins at both 1100 °C and 1150 °C were investigated with the help of a SEM.

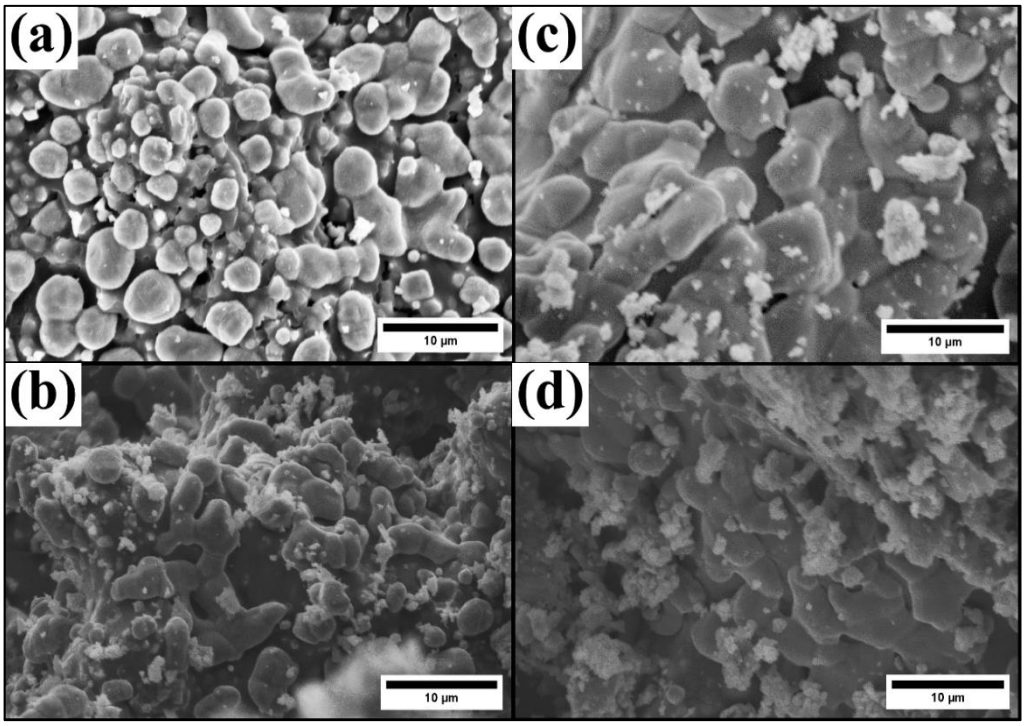

Figure 4.8: SEM micrographs of the pellet reduced with non-coking coal at (a) 1100 °C for 60 mins; (b) 1100 °C for 90 mins; (c) 1150 °C for 60 mins; and (d) 1150 °C for 90 mins.

Figure 4.8 shows the pellets reduced with non-coking coal. Individual small grains can be seen and some grains appear to have fused in **Figure 4.8a** which indicates the onset of sintering at 1100 °C and reduction time of 60 mins. Such small grains are not visible at reduction time of 90 mins **(Figure 4.8b)**. Smaller grains have already been replaced by large grains in **Figure 4.8c** which indicates that sintering had begun much earlier than the 60-minute mark. Similar sintering and fusion can be observed in **Figure 4.8d**. Similar behaviour was also seen in the SEM micrographs of pellets reduced with coke as shown in **Figure 4.9**. Little to no sintering is observed in **Figure 4.9a** while some grains appear to have sintered in **Figure 4.9c**, which indicates that the sintering process

had already begun at 60 mins for pellet reduced at 1150 °C. The extent of fusion and sintering was more in **Figure 4.9d** than in **Figure 4.9b** as the amount of smaller individual grains are more in **Figure 4.9b**.

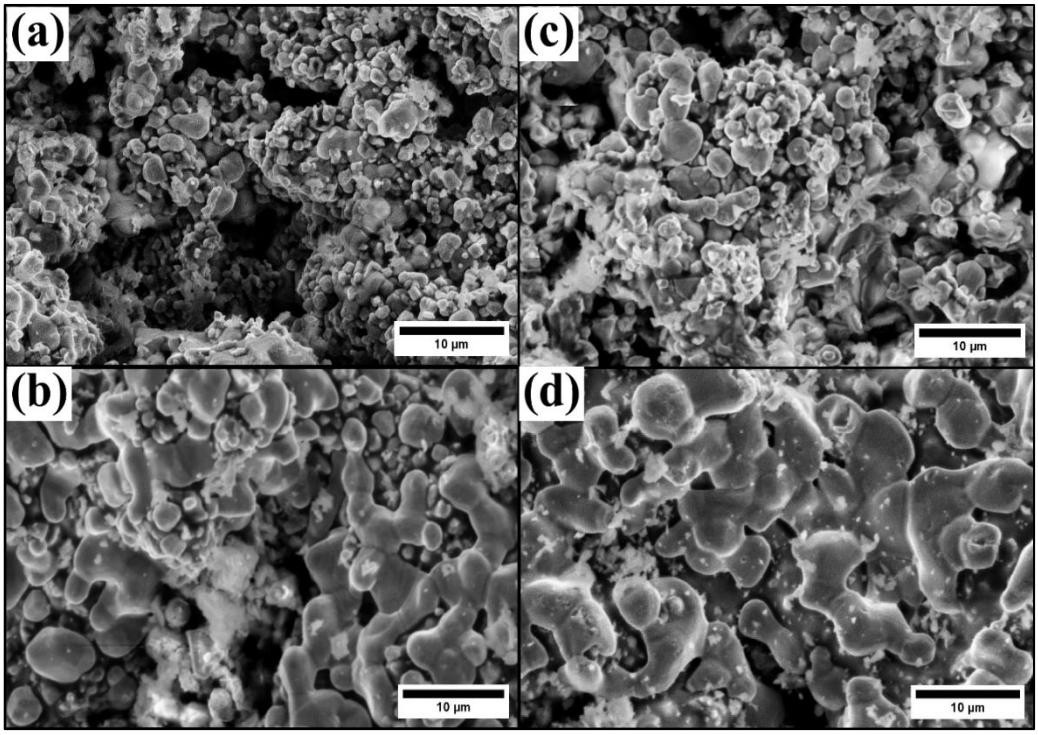

Figure 4.9: SEM micrographs of the pellet reduced with coke at (a) 1100 °C for 60 mins; (b) 1100 °C for 90 mins; (c) 1150 °C for 60 mins; and (d) 1150 °C for 90 mins.

Figure 4.10 shows the rate of reduction and rate of metallization of pellets reduced with coal and coke at both 1100 °C and 1150 °C. The metallic iron formation rate in the initial 60 mins for both non coking coal and coke is more at 1150 °C than at 1100 °C. Initially, the amount of metallic phase formed at 1150 °C was higher than at 1100 °C, sintering might have led to the formation of a dense, impervious layer at 1150 °C, and the thickness of the layer might have been more at 1150 °C than at 1100 °C. This would have resulted in increased resistance to diffusion of reducing gases in pellets reduced at 1150 °C than the pellets reduced at 1100 °C. Thus, with an increase in reduction time (> 60 mins), the reduction rate decreased, and reduction became more sluggish in the case of pellets reduced at 1150 °C, and % R became almost constant. Since the pellets

reduced at 1100 °C possessed more porosity than pellets reduced at 1150 °C, the % R increased progressively with increase in reduction times of more than 60 mins.

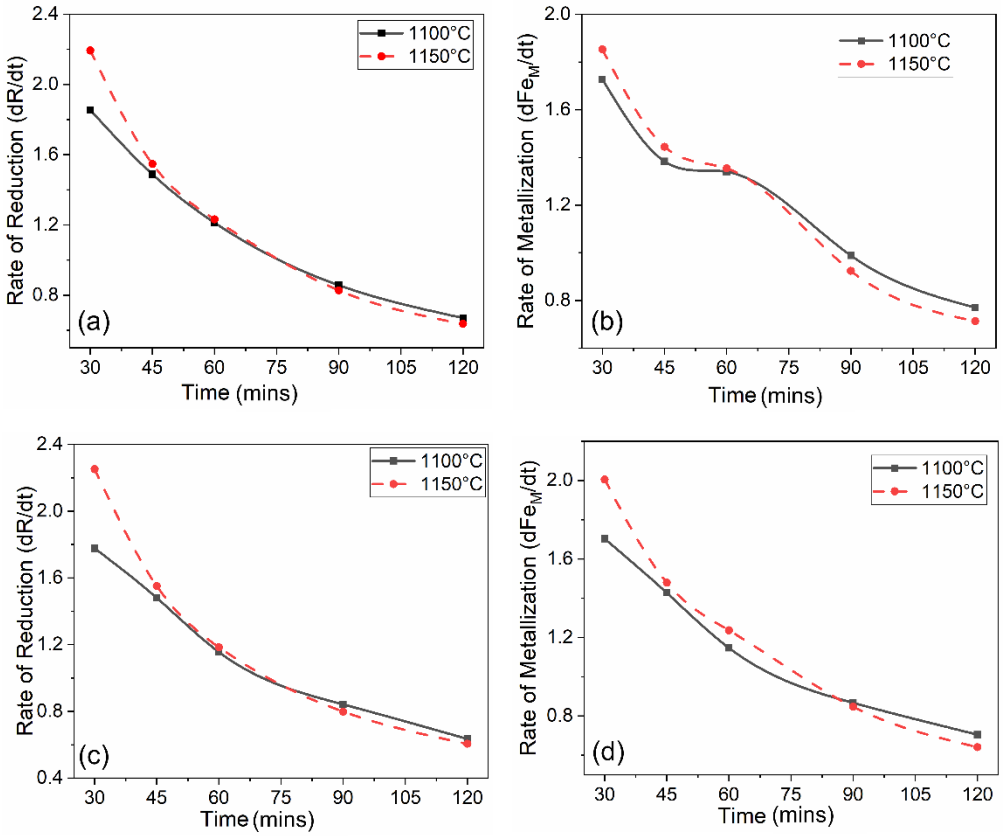

Figure 4.10: Variation in rate of reduction and rate of metallization with non coking coal (a & b); coke (c & d) as a reductant

4.2.5. Kinetic Studies

The reduction and subsequent metallization decreased beyond 1100 °C. Thus, the focus of further investigations was limited to the temperature range of 950-1100 °C. Experimental data were fitted to some existing reduction models to understand the kinetics and evaluate activation energy for the reduction reaction of MMO pellets. The % R values (in fraction form) were substituted in place of α (**Table 4.5**) in the equations to get model values. The plots of model values (**Table 4.6**) vs time for each model used, gave R^2 (rsqr) values which are shown in **Figure 4.11 and 4.12**. The R^2 (rsqr) values are a measure of how well the data fits a given model. The model with rsqr closest to 1 for all temperatures was assumed as the best fit model (**Table 4.7**). Activation energy was calculated by using the Arrhenius equation, for which the values of constant k are required. The slope of the lines of the best fit models was used as the constant k values. Six models were used for model fitting (**Table 4.5**)[98]

Table 4.5: Models used for fitting experimental data

Model Name	**Equation**
Chemical: Gasification control model equation	$-\ln(1-\alpha) = kt$
Phase-boundary-controlled reaction (contracting sphere)	$1-(1-\alpha)^{1/3}=kt$
Three-dimensional diffusion (Jander equation)	$[1-(1-\alpha)^{1/3}]^2 = kt$
Three-dimensional diffusion (Ginstling–Brounshtein equation)	$1-(2/3)\,\alpha-(1-\alpha)^{2/3} = kt$
Diffusion: Zhuravlev-Lesokhin-Tempel'man (ZLT) diffusion control model equation	$[(1-\alpha)^{-1/3}-1]^2 = kt$
Three-dimensional growth of nuclei (Avrami–Erofeyev equation)	$[-\ln(1-\alpha)]^{1/3}=kt$
α : fraction of reduction; **k** : slope of plotted lines; **t** : time consumed in reduction	

Table 4.6: Model values obtained for all kinetic models

Model Values							
Reductant	**Model**	**Temp (°C)**	**Time (mins)**				
			30	**45**	**60**	**90**	**120**
Non coking coal	$-\ln(1-\alpha) = kt$	950	0.314	0.448	0.613	0.729	0.754
		1000	0.652	0.781	0.778	1.005	1.214
		1050	0.818	1.105	1.133	1.43	1.563
		1100	0.813	1.108	1.302	1.475	1.632
	$1-(1-\alpha)^{1/3}=kt$	950	0.099	0.139	0.185	0.216	0.222
		1000	0.195	0.229	0.229	0.285	0.333
		1050	0.239	0.308	0.315	0.379	0.406
		1100	0.237	0.309	0.352	0.388	0.42
	$[1-(1-\alpha)^{1/3}]^2 = kt$	950	0.01	0.019	0.034	0.047	0.049
		1000	0.038	0.052	0.052	0.081	0.111
		1050	0.057	0.095	0.099	0.144	0.165
		1100	0.056	0.095	0.124	0.151	0.176
	$1-(2/3)\ \alpha-(1-\alpha)^{2/3} = kt$	950	0.009	0.017	0.03	0.04	0.042
		1000	0.033	0.044	0.044	0.066	0.086
		1050	0.048	0.075	0.078	0.107	0.12
		1100	0.047	0.076	0.095	0.112	0.127
	$[(1-\alpha)^{-1/3}-1]^2 = kt$	950	0.012	0.026	0.051	0.076	0.082
		1000	0.059	0.088	0.088	0.158	0.249
		1050	0.098	0.198	0.211	0.373	0.467
		1100	0.097	0.2	0.295	0.403	0.522
	$[-\ln(1-\alpha)]^{1/3}=kt$	950	0.68	0.77	0.85	0.9	0.91
		1000	0.87	0.92	0.92	1	1.07
		1050	0.94	1.03	1.04	1.13	1.16
		1100	0.93	1.03	1.09	1.14	1.18
Coke	$-\ln(1-\alpha) = kt$	950	0.368	0.444	0.527	0.648	0.658
		1000	0.519	0.631	0.719	0.896	1.042
		1050	0.9	1.04	1.114	1.174	1.238
		1100	1.001	1.097	1.182	1.417	1.435
	$1-(1-\alpha)^{1/3}=kt$	950	0.115	0.137	0.161	0.194	0.197
		1000	0.159	0.19	0.213	0.258	0.293
		1050	0.259	0.293	0.31	0.324	0.338
		1100	0.284	0.306	0.326	0.376	0.38
	$[1-(1-\alpha)^{1/3}]^2 = kt$	950	0.013	0.019	0.026	0.038	0.039
		1000	0.025	0.036	0.045	0.067	0.086
		1050	0.067	0.086	0.096	0.105	0.114
		1100	0.08	0.094	0.106	0.142	0.144
	$1-(2/3)\ \alpha-(1-\alpha)^{2/3} = kt$	950	0.012	0.017	0.023	0.033	0.034
		1000	0.023	0.031	0.039	0.055	0.069
		1050	0.056	0.069	0.076	0.082	0.089
		1100	0.065	0.075	0.083	0.106	0.108
	$[(1-\alpha)^{-1/3}-1]^2 = kt$	950	0.017	0.025	0.037	0.058	0.06
		1000	0.036	0.055	0.073	0.121	0.172
		1050	0.122	0.172	0.202	0.229	0.261
		1100	0.157	0.195	0.233	0.364	0.376
	$[-\ln(1-\alpha)]^{1/3}=kt$	950	0.72	0.76	0.81	0.87	0.87
		1000	0.8	0.86	0.9	0.96	1.01
		1050	0.97	1.01	1.04	1.05	1.07
		1100	1	1.03	1.06	1.12	1.13

The plots of model values vs time for non coking coal and coke are shown in **Figure 4.11** and **4.12** respectively.

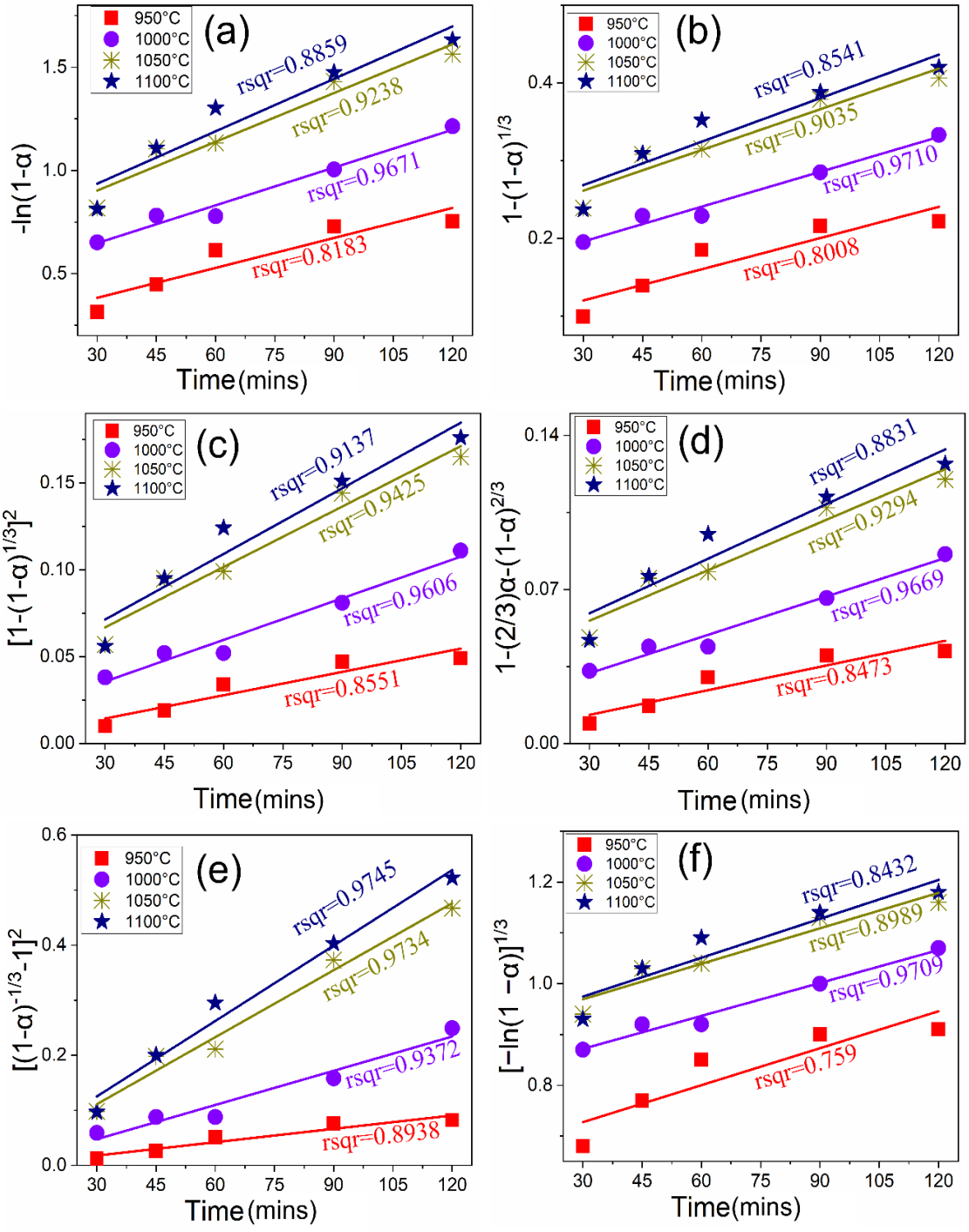

Figure 4.11: Plots of model versus time along with rsqr values for non-coking coal reduced pellets

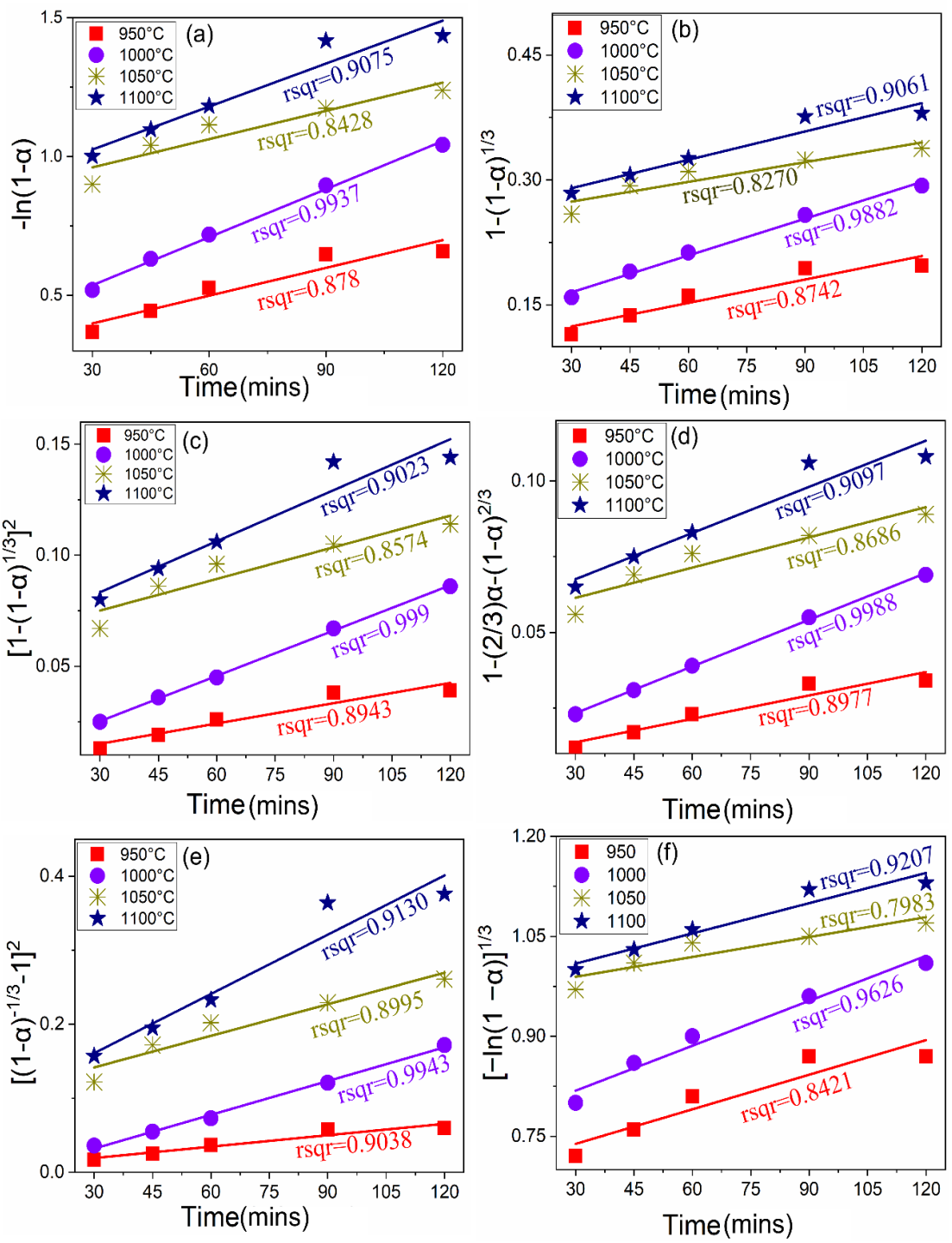

Figure 4.12: Plots of model versus time along with rsqr values for coke reduced pellets

The R^2(rsqr in the graphs) of the fitted data points in all the graphs are also mentioned in **Table 4.8**. From **Table 4.8** it can be seen that the kinetic model "$[(1-\alpha)^{-1/3}-1]^2 = kt$" was found to be the best fit as the rsqr were closest to 1 for both non coking coal and coke. In this model, the diffusion of one reactant through the layer between the two reactants controls the reaction rate [98]. The model is known as the Zhuravlev-Lesokhin-Tempel'man (ZLT) diffusion control model which is a variation of the Jander equation and it is assumed that one of the reactants completely surrounds the other spherical reactant. The surrounding reactant has to pass through the layer separating both reactants. In this case, the reaction between non coking coal/coke and ore/pellet is controlled by boundary layer diffusion. The rate of the overall reaction is determined by the transport of gaseous reactants and products through a thin boundary layer surrounding the solid particles. Gaseous reactants such as CO and H_2, generated from coal or coke, diffuse through this boundary layer to reach the reaction sites on the surface of the pellet. Simultaneously, gaseous products like CO_2 and H_2O, formed as a result of the reduction reaction, diffuse away from the reaction sites through the same boundary layer.

Initially, the boundary layer is between the oxide (Fe_2O_3) and the ambient air. As reduction proceeds and products like Fe_3O_4, FeO, and Fe form, the boundary layer shifts to the interfaces between these different phases: Fe-FeO, FeO- Fe_3O_4, and Fe_3O_4 - Fe_2O_3. The reducing gases (CO, H_2) diffuse inward toward the center of the pellet through these boundary layers, while the product gases (CO_2, H_2O) diffuse outward toward the ambient air through the same boundary layers. This diffusion process through the boundary layer dictates the overall reaction rate.

Table 4.7: R^2 (rsqr) values of all fitted curves in Figures 4.13 and 4.14

R^2 values					
Reductant	**Model**	**Temperature(°C)**			
		950	1000	1050	1100
Non coking Coal	$-\ln(1-\alpha) = kt$	0.8183	0.9671	0.9238	0.8859
	$1-(1-\alpha)^{1/3} = kt$	0.8008	0.9710	0.9035	0.8541
	$[1-(1-\alpha)^{1/3}]^2 = kt$	0.8551	0.9606	0.9425	0.9137
	$1-(2/3)\,\alpha-(1-\alpha)^{2/3} = kt$	0.8473	0.9669	0.9294	0.8831
	$[(1-\alpha)^{-1/3}-1]^2 = kt$	0.8938	0.9372	0.9734	0.9745
	$[-\ln(1-\alpha)]^{1/3} = kt$	0.7590	0.9709	0.8989	0.8432
Coke	$-\ln(1-\alpha) = kt$	0.8780	0.9937	0.8428	0.9075
	$1-(1-\alpha)^{1/3} = kt$	0.8742	0.9882	0.8270	0.9061
	$[1-(1-\alpha)^{1/3}]^2 = kt$	0.8943	0.9990	0.8574	0.9023
	$1-(2/3)\,\alpha-(1-\alpha)^{2/3} = kt$	0.8977	0.9988	0.8686	0.9097
	$[(1-\alpha)^{-1/3}-1]^2 = kt$	0.9038	0.9943	0.8995	0.9130
	$[-\ln(1-\alpha)]^{1/3} = kt$	0.8421	0.9626	0.7983	0.9207

The slope values of the fitted lines in **Figure 4.11e and 4.12e** were taken as constant k values to calculate activation energy of the reduction process. The constant k values are reported in **Table 4.8**. Arrhenius equation was used to calculate activation energy.

The arrhenius equation is given as

$$k = Ae^{-E_a/RT} \quad \text{.....4.9}$$

where k = rate constant of the reaction
A= pre-exponential factor
E_a =activation energy of the chemical reaction
R= universal gas constant
T= absolute temperatures in Kelvin

Taking logarithm on both sides of eqn gives

$$\ln k = \left(\frac{-E_a}{RT}\right)\left(\frac{1}{T}\right) + const$$

The above equation resembles the general form of a linear equation

$$y = mx + c$$

Thus, if a graph is plotted with ln k values in y axis and and 1/T values in x axis, then the slope of the line obtained will be equal to ($-E_a/R$) which on further simplification gives the the value of activation energy E_a.

Table 4.8: Activation energy with non coking coal and coke as a reductant

Activation Energy Calculation						
Reductant	**Temp(°C)**	**k-values**	**ln k**	**1/T*10^4 (K^{-1})**	**Slope**	**Activation energy (KJ/mol)**
Non coking coal	950	0.00081	-7.118	8.176	-1.989	165.382
	1000	0.00207	-6.180	7.855		
	1050	0.00406	-5.506	7.558		
	1100	0.00457	-5.388	7.283		
Coke	950	0.00051	-7.573	8.176	-2.648	220.194
	1000	0.00152	-6.489	7.855		
	1050	0.00142	-6.557	7.558		
	1100	0.00267	-5.925	7.283		

Figure 4.13 shows the arrhenius plot for both non coking coal and coke. The slope of the fitted line is mentioned in the figure itself.

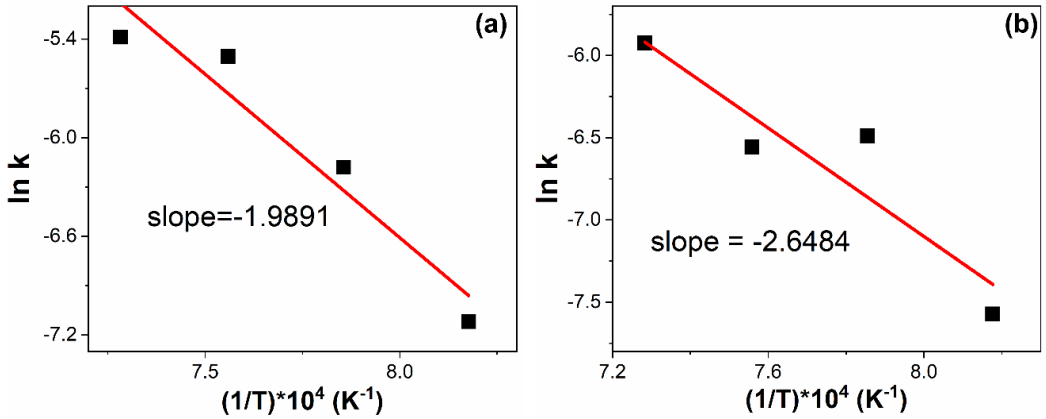

Figure 4.13: Arrhenius plot for reductants: (a) non-coking coal and (b) coke

The reduction of the pellets was found to be diffusion controlled irrespective of the reductant used. The decrease in porosity due to sintering (**Figures 4.8 and 4.9**) decreased the reduction rate, indicating that the gas diffusion into the pellet through the

metallic layer might have become difficult. Thus, diffusion of CO into the pellet controlled the overall rate of reaction, which is in line with the suggested mechanism of the best fit model.

The activation energy was found to be ~165.38 KJ/mole for pellets reduced with non coking coal and ~220.195 KJ/mole for pellets reduced with coke. This value was similar to that reported by Chakraborty et al [99] for hematite (138 KJ/mole) and chromite (172 KJ/mole) for carbothermic reduction of chromite ore. The activation energy of this MMO was also within the range of other MOs like Ti-Fe ores, whose activation energy was 93.42-179.80 KJ/mol at 1000-1200 °C [44], and of carbothermic reduction of V-Ti-Magnetite ores (88.7-295 KJ/mol) [43]. The activation energy for the reduction of MMO pellets using non-coking coal is lower compared to that obtained with coke. This difference is attributed to the higher volatile matter (VM) content in non-coking coal (9.21%) compared to coke (2.1%). Volatile matter typically begins to break down into CO and H_2 around 700 °C [100] leading to pre-reduction of the pellet even before the reduction temperatures of 950°C used in the present investigations are reached [101]. The VM content of non-coking coal was higher than that of coke, the reduction process was initiated earlier and facilitated by the presence of the reducing gases (H_2 and CO from the VM), resulting in a lower subsequent activation energy.

4.3. Conclusions

The reduction and its kinetics for pellets made from MMO fines was studied between 950-1150 °C with two solid reductants: non coking coal and coke. The following conclusions were drawn.

- At a reduction temperature of 1100°C and a reduction time of 90 mins, pellets reduced with non-coking coal yielded a desired $\%Fe_M$ of greater than 85%.
- Pellets reduced with coke attained a maximum %R of 76% and maximum $\%Fe_M$ of 83% at 1100°C with a reduction time of 120 mins. However, this metallization did not meet the minimum industrial standards requirement of 85%
- At 1100°C, the %R after 60 mins was higher than at 1150°C for both non-coking coal-reduced and coke-reduced pellets. XRD analysis of MMO pellets reduced at both temperatures revealed no major phase change. SEM analysis indicated a higher degree of sintering in pellets reduced at 1150°C, resulting in decreased porosity. This reduced porosity increased the resistance to gas flow to the pellets' inner core, thereby affecting the subsequent %R.
- The kinetic model $[(1-\alpha)^{-1/3}-1]^2 = kt$ was observed to be the best fit for the reduction of MMO pellets regardless of the reductant used. The calculated activation energy was approximately 165.38 KJ/mole for non-coking coal reduced pellets and 220.19 KJ/mole for coke-reduced pellets. It shows that non coking coal was a better reductant than coke.